

Phonon heat conduction in micro- and nano-core-shell structures with cylindrical and spherical geometries

Taofang Zeng and Wei Liu

Citation: [Journal of Applied Physics](#) **93**, 4163 (2003); doi: 10.1063/1.1556566

View online: <http://dx.doi.org/10.1063/1.1556566>

View Table of Contents: <http://scitation.aip.org/content/aip/journal/jap/93/7?ver=pdfcov>

Published by the [AIP Publishing](#)

Articles you may be interested in

[Anomalous thermal conductivity by surface phonon-polaritons of polar nano thin films due to their asymmetric surrounding media](#)

J. Appl. Phys. **113**, 084311 (2013); 10.1063/1.4793498

[Thermodynamic characterization of the diffusive transport to wave propagation transition in heat conducting thin films](#)

J. Appl. Phys. **112**, 123707 (2012); 10.1063/1.4769430

[Strain effect analysis on phonon thermal conductivity of two-dimensional nanocomposites](#)

J. Appl. Phys. **106**, 114302 (2009); 10.1063/1.3259383

[Nanoscale thermal transport](#)

J. Appl. Phys. **93**, 793 (2003); 10.1063/1.1524305

[Phonon heat conduction in a semiconductor nanowire](#)

J. Appl. Phys. **89**, 2932 (2001); 10.1063/1.1345515



Phonon heat conduction in micro- and nano-core-shell structures with cylindrical and spherical geometries

Taofang Zeng^{a)}

Mechanical and Aerospace Engineering Department, North Carolina State University, Raleigh, North Carolina 27695

Wei Liu

Power Engineering Department, Huazhong University of Science and Technology, Wuhan 430074, People's Republic of China

(Received 17 May 2002; accepted 9 January 2003)

This study examines the definition of temperatures at interfaces and within thin films when the phonons are in nonequilibrium, and provides a general solution for the temperature distribution within the micro- and nanocylindrical and spherical shells. By applying the Boltzmann transport equation and the established methods of thermal radiation heat transfer, analytical solutions for the temperature distribution and equivalent thermal conductivity are obtained for micro- and nanocylindrical and spherical shells. The study shows that significant drops in temperature occur at the interfaces of micro- and nanocylindrical and spherical shells. For cylindrical shells, the effective thermal conductivity is determined by both the film thickness and the diameter of the inner cylinder. For spherical shells, the effective conductivity is mainly determined by the size of the inner sphere.

© 2003 American Institute of Physics. [DOI: 10.1063/1.1556566]

I. INTRODUCTION

Heat conduction in dielectric or semiconductor thin films has attracted intensive attention in the last decade. It is now well accepted that when the film thickness becomes comparable to, or smaller than, the phonon mean free path, the size effect and interface effect become significant, and the Boltzmann transport equation should be and can be applied to describe phonon transport. In Refs. 1–6 are some examples on phonon heat conduction in thin film heterostructures and superlattices.

It should be noted that all the previous studies have largely focused on planar thin films. Nonetheless, a wide range of micro- and nanoscale thermal problems is associated with nonplanar geometries such as spherical and cylindrical media, and they have not been studied. With the rapid growth of research and development of nanomaterials and nanostructures,⁷ understanding of heat transfer in micro- and nanocylindrical and spherical media becomes important. Examples include semiconductor nanowires coated with a redox layer⁸ and carbon-sheathed nanowires,⁹ and three-dimensional microstructures.¹⁰ In these devices and structures, the nano- and microcylinders are coated with another thin layer of materials. SiO₂-coated Fe nanoparticles¹¹ and oxide capped CdSe nanoparticles¹² are good examples of nanosized core-shell structures.

The object of the present study is a thin shell sandwiched between two concentric cylinders and spheres, representing nonplanar structures mentioned above (shown in Fig. 1). For those micro- and nanostructures, the size effect of thermal conductivity is dependent on structural geometries within the Casimir limit.¹³ The nonequilibrium phonons are first dis-

cussed, and the definition of temperatures at interfaces is then examined. By applying the Boltzmann transport equation and established methods of thermal radiation heat transfer, an analytical solution for the temperature distribution and equivalent thermal conductivity is obtained. The study shows that significant drops in temperature occur at the interfaces, and the phonon transmission and reflection is the dominant factor for determining the equivalent thermal conductivity of micro- and nanocylindrical and spherical media.

II. PHYSICAL MODELS AND METHODS OF SOLUTION

Consider a micrometer to nanometer scale medium with cylindrical and spherical geometry, shown in Figs. 1(a) and 1(b). The object of this study is the layer between the core and the sheaths—the inner cylinder and the outer cylinder in Fig. 1(a), and the inner sphere and the outer sphere in Fig. 1(b). To include the effect of the core on heat conduction inside the film and thermal boundary resistance, while excluding the complication of the heat conduction process in the bulk core material, it is assumed that phonons are emitted at uniform temperature from the core and the sheath and travel towards the interface. These phonons can be thought of as coming from the core side within one mean free path.⁴ Phonon transport in the core or the sheath beyond one mean free path can be treated based on Fourier heat conduction theory. This study mainly deals with phonon transport, and details of the phonon scattering mechanism are omitted and represented by an average mean free path.^{2–4} Under these approximations, and with the intensity representation,² the Boltzmann transport equation can be written as

$$\mu \frac{\partial I}{\partial r} + \frac{1 - \mu^2}{r} \frac{\partial I}{\partial \mu} = \frac{I^0 - I}{\Lambda} \quad (\text{in spherical coordinates}), \quad (1a)$$

^{a)}Electronic mail: tzeng2@unity.ncsu.edu

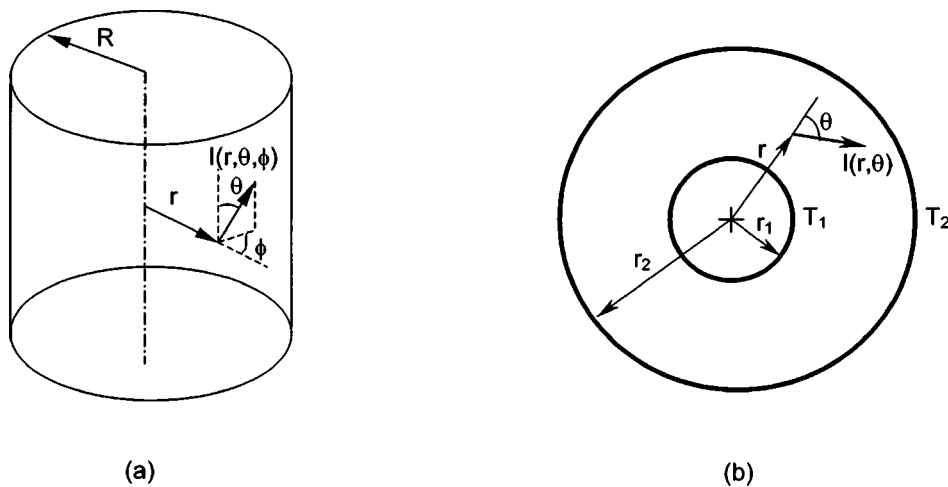


FIG. 1. (a) Coordinates for cylindrical symmetry; (b) coordinates for spherical symmetry.

$$\sin \theta \left[\cos \phi \frac{\partial I(r, \theta, \phi)}{\partial r} - \frac{\sin \phi}{r} \frac{\partial I(r, \theta, \phi)}{\partial \phi} \right] = \frac{I^0 - I}{\Lambda} \quad (\text{in cylindrical coordinates}), \quad (1b)$$

where I is the total phonon intensity, I^0 the equilibrium phonon intensity approximated as

$$I^0 = \frac{1}{4\pi} C \nu (T - T_{\text{ref}}) + I_{\text{ref}}^0. \quad (2)$$

where Λ is the phonon average mean free path, θ the polar angle, ϕ the azimuthal angle, $\mu (= \cos \theta)$ the directional cosine, I_{ref}^0 the equilibrium phonon intensity at the reference point, C the specific heat, and ν the magnitude of the phonon group velocity. It should be emphasized that Eq. (2) is valid only when C is temperature independent, and the temperature in Eq. (2) may represent a highly nonequilibrium situation and it is best regarded as a quantity that represents the local total phonon energy.

The above equations are the same as thermal radiation equations with isotropic scattering. The solutions are well documented in the literature on heat transfer.^{14,15} The exact solutions are, however, quite complicated even for simplified cases. Instead, some approximate solutions are generally used. One method used most is the optically thick approximation coupled with Deissler's jump boundary conditions. The solution is close to the exact solution for planar geometries.^{14,15} The same results apply to phonon transport around nanoparticles.¹⁶ It also has been shown that the optically thick approximation gives almost the same results as those by directly solving the Boltzmann transport equation for both electrons and phonons.^{4,17} The basic idea behind this approach is the diffusion or quasiequilibrium approximation within the medium.

In thermal radiation, it is believed that the diffusion approach works for planar structures, but not for other structures including cylindrical and spherical shapes.¹⁵ Phonon transfer in thin films with cylindrical and spherical geometries is, however, a special case for a general solution of the thermal radiation transport equation or the Boltzmann transport equation in cylindrical and spherical coordinates: The

phonon scattering rate is fixed, and so is the mean free path; whereas, in thermal radiation the optical path length is determined by both the photon radiation mean free path and the gap between the two concentric cylinders and spheres. Equations (9–57) in Ref. 14 demonstrate that when the gap is zero or close to zero ($r_1 = r_2$, or $r_1 \rightarrow r_2$), the diffusion approximation works for thermal radiation in the medium between two concentric cylindrical spheres. For phonon transport in thin films, $r_1 \rightarrow r_2$, which allows the diffusion approximation to work. Calculation results in Sec. III further validate the approximation. Here in Sec. II, we establish the analytical formulation for phonon transport.

By applying the diffuse approximation, quasiequilibrium phonon distribution in the film, the phonon intensity within nanocylindrical media can be expressed as

$$I = I^0 - \sin \theta \left[\cos \phi \frac{\partial I^0(r)}{\partial r} - \frac{\sin \phi}{r} \frac{\partial I^0(r)}{\partial \phi} \right] \Lambda = I^0 - \sin \theta \cos \phi \frac{\partial I^0(r)}{\partial r}. \quad (3)$$

This equation applies for both the micro- and nanomedium and the outer layer and the inner layer surrounding the medium. The heat flux along the radial direction is

$$\begin{aligned} q(r) &= \int_0^{2\pi} I d\Omega_r \\ &= \int_0^{2\pi} I \sin \theta \cos \phi d\Omega = \int_0^{2\pi} I \sin^2 \theta \cos \phi d\theta d\phi \\ &= -2 \int_{\phi=0}^{2\pi} \cos^2 \phi d\phi \int_0^\pi \sin^3 \theta d\theta \cdot \Lambda \frac{dI^0}{dr} \\ &= -\frac{4\pi}{3} \Lambda \frac{dI^0}{dr} = -\frac{1}{3} C \nu \Lambda \frac{dT}{dr}. \end{aligned} \quad (4)$$

This is nothing but Fourier's law. The difference compared to the traditional way of applying Fourier's law comes from the boundary conditions.

As shown in Fig. 2, at interfaces, phonons can be transmitted into another material and can also be reflected back to

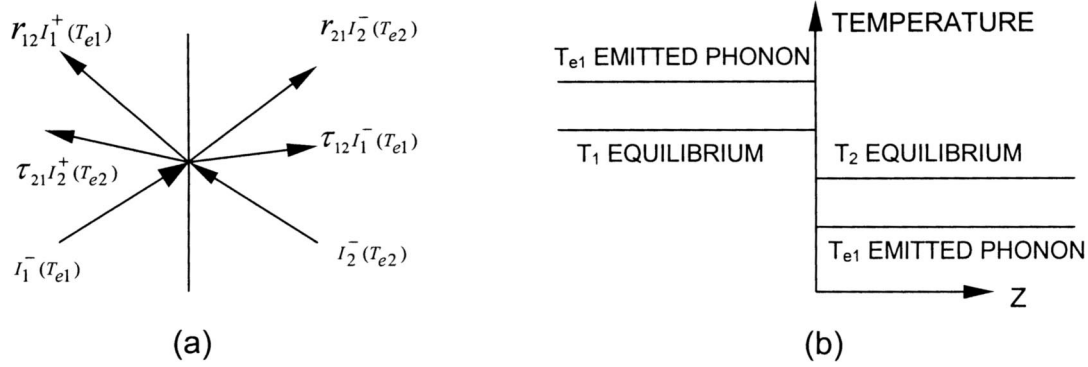


FIG. 2. Phonon transport at one interface: (a) incident, reflected, and transmitted phonons and (b) the temperature on each side of the interface.

the emitter itself. As a result of phonon transmission and reflection, there exists an equilibrium phonon temperature T_i , whereas T_{ei} is the temperature of the emitting phonons. The heat flux across the interface at $r=r_1$ in Fig. 2 can be written as

$$q(r_1) = \int \tau_{12}I_1(r_1)d\Omega_r - \int \tau_{21}I_2(r_1)d\Omega_r, \quad (5)$$

where I_1 is the effective equilibrium phonon intensity in the reservoir (core), and τ_{ij} is the transmissivity. Note that the solid angle ($d\Omega$) in the r direction is $d\Omega_r = \sin \theta \cos \phi d\Omega$, and $\Omega_r = [0, 2\pi]$, or $\phi = [-\pi/2, \pi/2]$, $\theta = [0, \pi]$. The principle of energy balance, i.e., the net heat flux, must be zero when $I_1(r_1) = I_2(r_1)$, leads to the following expression:

$$\int \tau_{12}I_1(r_1)d\Omega_r = \int \tau_{21}I_2(r_1)d\Omega_r.$$

Therefore, Eq. (5) can be written as

$$q(r_1) = \int \tau_{21}[I_1(r_1) - I_2(r_1)]d\Omega_r. \quad (6)$$

Substituting Eq. (3) into Eq. (6) for both $I_1(r_1)$ and $I_2(r_1)$ and noticing the opposite direction of the coordinates for them yields

$$\begin{aligned} q(r_1) = & \int \tau_{21}[I_1^0(T_{r=r_1}) - I_2^0(T_{r=r_1})]d\Omega_r \\ & + \Lambda \frac{dI_1^0}{dx} \int \tau_{12} \sin \theta \cos \phi d\Omega_r \\ & + \Lambda \frac{dI_2^0}{dx} \int \tau_{21} \sin \theta \cos \phi d\Omega_r, \end{aligned} \quad (7)$$

or

$$\left(1 - \frac{\tau'_{12} + \tau'_{21}}{2}\right) q(r_1) = \frac{Cv\tau''_{21}}{4}(T_1 - T_{r=r_1}), \quad (8)$$

where the average transmissivities τ'_{12} , τ'_{21} , and τ''_{21} are defined as

$$\tau'_{21} = \frac{3}{2\pi} \int_0^\pi \tau_{21} \sin \theta \cos \phi d\Omega_r,$$

$$\tau'_{12} = \frac{3}{2\pi} \int_0^\pi \tau_{12} \sin \theta \cos \phi d\Omega_r, \quad (9)$$

$$\tau''_{21} = \frac{1}{\pi} \int_0^\pi \tau_{21} d\Omega_r. \quad (10)$$

Similarly, at $r=r_2$, one can have

$$\left(1 - \frac{\tau'_{23} + \tau'_{32}}{2}\right) q(r_2) = \frac{Cv\tau''_{32}}{4}(T_{r=r_2} - T_2). \quad (11)$$

Let $q(r)$ be the net heat flux at any radial location r . The total net radial heat transfer Q in the radial direction per unit length of the cylinder is

$$Q = 2\pi r q(r) = \text{const.} \quad (12)$$

Then Eq. (4) can be rearranged as

$$\frac{dT}{dr} = - \frac{3}{Cv\Lambda} \frac{Q}{2\pi r}. \quad (13)$$

Integrating this equation gives

$$T(r) - T(r_1) = - \frac{3}{2\pi} \frac{Q}{Cv\Lambda} \ln\left(\frac{r}{r_1}\right), \quad (14a)$$

$$T(r_2) - T(r_1) = - \frac{3}{2\pi} \frac{Q}{Cv\Lambda} \ln\left(\frac{r_2}{r_1}\right). \quad (14b)$$

Equations (8) and (11) can be rearranged as

$$T(r_1) = T_1 - \frac{4}{Cv\tau''_{21}} \left(1 - \frac{\tau'_{21} + \tau'_{12}}{2}\right) \frac{Q}{2\pi r_1}, \quad (15a)$$

$$T(r_2) = T_2 + \frac{4}{Cv\tau''_{23}} \left(1 - \frac{\tau'_{23} + \tau'_{32}}{2}\right) \frac{Q}{2\pi r_2}, \quad (15b)$$

Combining Eqs. (14b), (15a), and (15b) results in

$$Q_{\text{cylinder}} = \frac{1}{3} C v \Lambda (T_1 - T_2) \cdot (3 \pi r_1 / 2 \Lambda) \cdot \frac{1}{[1 - (\tau'_{21} + \tau'_{12})/2] / \tau''_{21} + [1 - (\tau'_{23} + \tau'_{32})/2] / \tau''_{23} \cdot r_1 / r_2 + (3 r_1 / 4 \Lambda) \ln(r_2 / r_1)}. \quad (16)$$

For bulk materials, the third term $[(3 r_1 / 4 \Lambda) \ln(r_2 / r_1)]$ in the denominator dominates since $r_1 \gg \Lambda$, and Eq. (16) reduces to traditional Fourier law. The other two terms are important when the core cylinder has a diameter comparable to the mean free path or when the shell layer thickness is comparable to the mean free path. In the same way, the heat flux for concentric spherical micro- and nanomedia can be written as

$$Q_{\text{sphere}} = \frac{1}{3} C v \Lambda (T_1 - T_2) \cdot (3 \pi r_1^2 / \Lambda) \cdot \frac{1}{[1 - (\tau'_{21} + \tau'_{12})/2] / \tau''_{21} + [1 - (\tau'_{23} + \tau'_{32})/2] / \tau''_{23} \cdot r_1^2 / r_2^2 + 3 r_1 / 4 \Lambda [1 - (r_1 / r_2)]}, \quad (17)$$

where $Q_{\text{sphere}} = 4 \pi r^2 q(r)$ is the total heat flux. The temperature distribution can then be found by using Eqs. (14) and (15) for cylindrical media. The same methods apply to spherical media. The equivalent thermal conductivity for the cylindrical and spherical media can be derived from

$$Q = \frac{2 \pi k_{\text{eff}} (T_1 - T_2)}{\ln(r_2 / r_1)} \text{ (cylindrical media)}, \quad (18a)$$

$$Q = \frac{4 \pi k_{\text{eff}} r_1 (T_1 - T_2)}{1 - r_1 / r_2} \text{ (spherical media)}. \quad (18b)$$

$$\frac{k_{\text{eff_cylinder}}}{k_{\text{bulk}}} = \frac{3 r_1 / 4 \Lambda}{\{[1 - (\tau'_{21} + \tau'_{12})/2] / \tau''_{21} + [1 - (\tau'_{23} + \tau'_{32})/2] / \tau''_{23} \cdot (r_1 / r_2)\} / [\ln(r_2 / r_1)] + (3 r_1 / 4 \Lambda)}, \quad (19)$$

$$\frac{k_{\text{eff_sphere}}}{k_{\text{bulk}}} = \frac{3 r_1 / 4 \Lambda}{\{[1 - (\tau'_{21} + \tau'_{12})/2] / \tau''_{21} + [1 - (\tau'_{23} + \tau'_{32})/2] / \tau''_{23} \cdot (r_1^2 / r_2^2)\} / [1 - r_1 / r_2] + (3 r_1 / 4 \Lambda)}. \quad (20)$$

Note that when $r_1 = r_2$, Eqs. (16) and (17) give the correct calculation for heat flux, which is determined by the thermal boundary resistance at the interface. In this situation, the equivalent thermal conductivity is zero, because the thermal resistance has a finite value, but the thickness of the layer is zero.

III. RESULTS AND DISCUSSION

In optical fibers, the core is generally made of silicon dioxide or silicates; the cladding is made of another type of glass; and the waveguides are coated with polymer. As an example of calculation, a system of silicon dioxide as the core and silicon as the nanomedium is studied here. This is different from the real structure, but it gives a clearer comparison. The physical properties are provided in Table I. The other important parameters are the transmittances of τ_{ij} at interfaces. This can be very complicated if the surface is partially specular and partially diffuse.^{3,4} In this calculation, the interfaces are assumed to be totally diffuse. The transmissivity is $\tau_{ij} = (C_j v_j / C_i v_i + C_j v_j)$.¹⁸

TABLE I. Parameters used in the calculation (from Ref. 16).

	Specific heat ($\times 10^6$ J/m ³ K)	Group velocity (m/s)	Mean free path (Å)	Density (kg/m ³)
SiO ₂	1.79	4100	6	2278
Si	1.64	6533	430	2330

Figures 3(a)–3(d) show the distribution of the dimensionless equilibrium temperature, $\Theta = (T - T_1) / (T_2 - T_1)$ for cylindrical and spherical media. Large drops in temperature occur at the interface due to the dissimilarity of the two materials when the thickness of the layer studied (thin film) and the size of the inner cylinder and sphere are smaller than or comparable to the mean free path [Figs. 3(a) and 3(b)]. When the thickness of the layer studied (thin film) and the size of the inner cylinder and sphere are larger than the mean free path [Figs. 3(c) and 3(d)], the temperature distribution is very close to that predicted by Fourier's law. This validates the approximation method in the study. The deviation from Fourier's law shows the propensity for nonequilibrium of the phonons. In this situation, the equivalent temperatures for the phonons are defined so as to represent the energy level. Within the film, continuation of the equivalent temperature or the phonon energy level demonstrates the uniformity or homogeneity of the materials structure.

When the film thickness is small compared to the mean free path, the phonon energy in the film is mainly determined by the incoming phonons transmitted through the interfaces which generates temperature discontinuity at the interface [Figs. 3(a) and 3(b)]. When the film thickness is large, phonons are at local equilibrium and isentropic in all directions, and the phonon energy level or the temperature is continuously distributed over the whole structure [Figs. 3(c) and 3(d)].

Figures 4(a) and 4(b) show the normalized thermal conductivity as a function of the normalized diameter of the

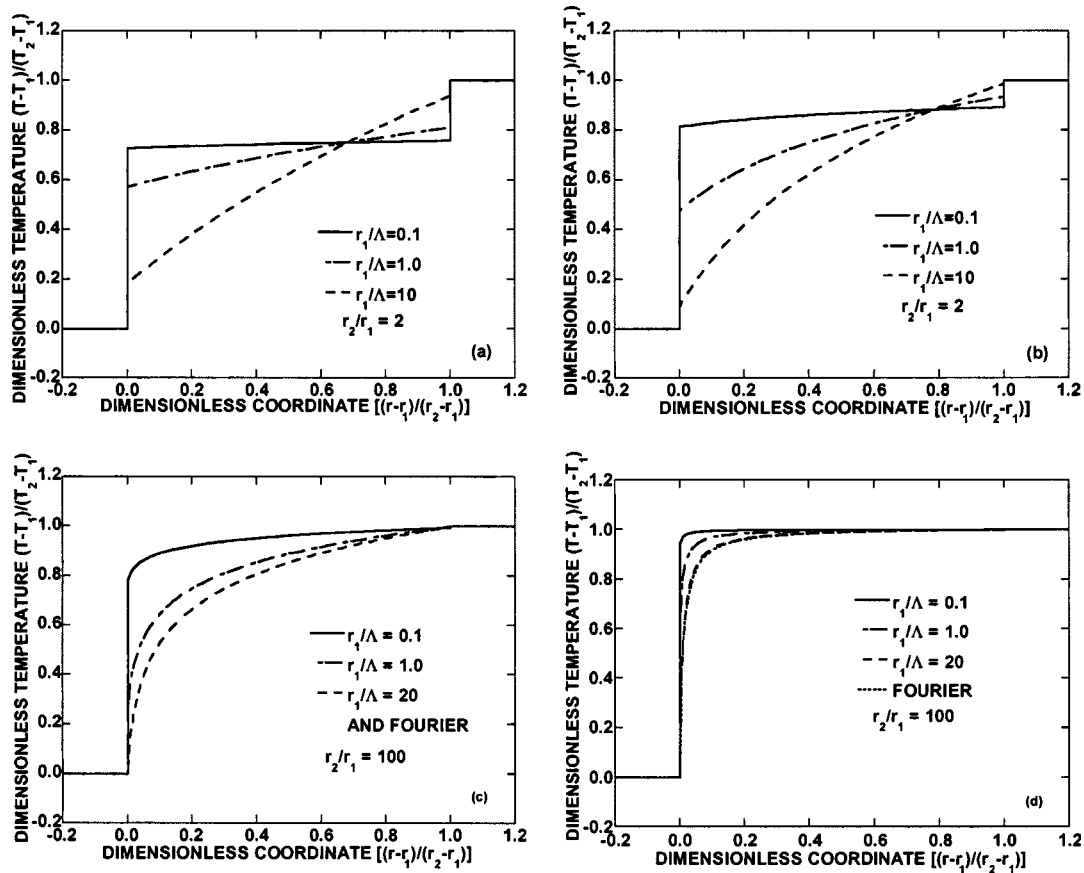


FIG. 3. Distribution of dimensionless temperatures in (a) cylindrical and (b) spherical media of thin films with $r_2/r_1=2$ and (c) cylindrical and (d) spherical media for bulk films with $r_2/r_1=100$.

cylinder and of the sphere for different film thicknesses ($\delta = r_2 - r_1$). Not surprisingly, the equivalent thermal conductivity approaches the value for bulk materials as the diameter increases. Figures 5(a) and 5(b) plot the equivalent thermal conductivity as a function of the film thickness for different diameters of the cylinders and spheres. It is interesting to note that when the diameter of the inner layer is very large (for example, $r_1/\Lambda = 100$), the equivalent thermal conductivity is basically independent of the film thickness, and it is very close to the value of the corresponding bulk materials.

In comparing Figs. 4(a) and 5(a), one finds that the effective thermal conductivity of cylindrical media is determined by both the diameter of the inner cylinder and by the thickness of the cladding layer, whereas for the spherical structure, the effective thermal conductivity is mainly dependent on the size of the inner particle, and the thickness of the cladding layer is a second-order factor [Figs. 4(b) and 5(b)]. One can thus let $r_2 \gg r_1$ and concentrate on studying the effect of sphere size. When $r_2 \gg r_1$, Eq. (20) reduces to

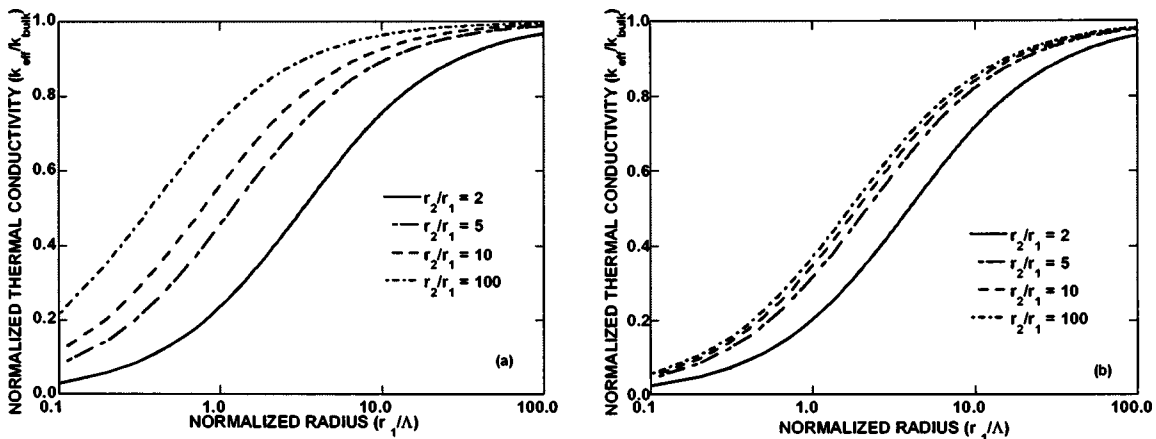


FIG. 4. Effective thermal conductivity for (a) cylindrical and (b) spherical media as a function of the diameter of the inner cylinder and the sphere.

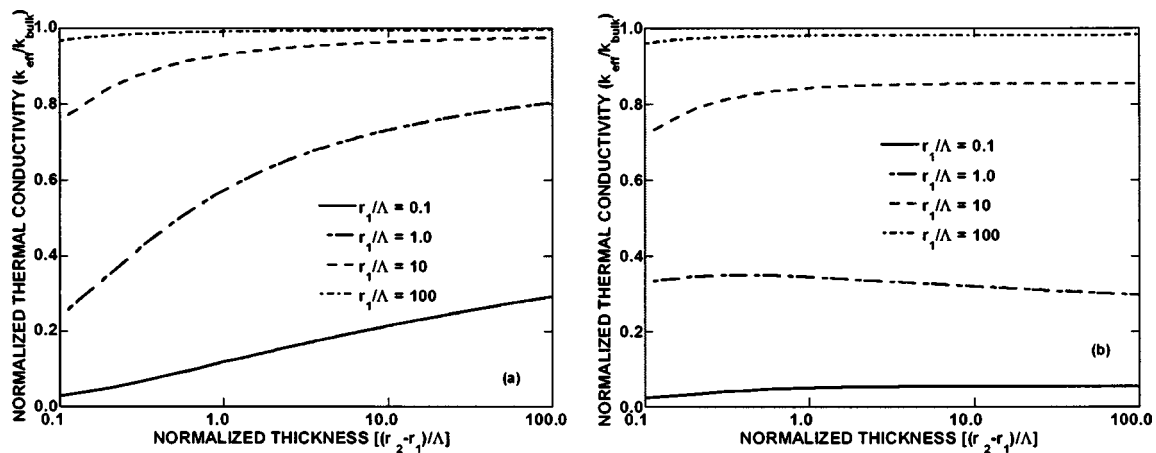


FIG. 5. Effective thermal conductivity for (a) cylindrical and (b) spherical media as a function of the film thickness.

$$\frac{k_{\text{eff}}}{k_{\text{bulk}}} = \frac{3r_1/4\Lambda}{[1 - (\tau'_{21} + \tau'_{12})/2]/\tau'''_{21} + 3r_1/4\Lambda}. \quad (21)$$

Furthermore, when $[1 - (\tau'_{21} + \tau'_{12})/2]/\tau'''_{21} = 1$, Eq. (21) becomes

$$\frac{k_{\text{eff}}}{k_{\text{bulk}}} = \frac{3r_1/4\Lambda}{1 + 3r_1/4\Lambda}. \quad (22)$$

This is the same expression as that in Chen's paper,¹⁶ where Eq. (22) is presented by experience fitting without justification. As has been shown, Eq. (22) is only a special situation for Eq. (21). Nonetheless, for this special situation, Chen's study¹⁶ showed that Eq. (22) provides almost the same results as that by the exact solution. This also validates the approximation in this study. The general validation of the method is as follows.

Diffusion approximation coupled with Deissler's jump boundary condition is a proven method for thermal radiation in planar geometries.¹⁵ However, it is generally believed that this method is not applicable for thermal radiation in cylindrical and spherical geometries. Its failure is demonstrated by Fig. 13-1 in Ref. 15. When the absorption coefficient k approaches zero, and so does the optical thickness, the non-dimensional heat flux approaches zero instead of one, the correct limit. On the other hand, if one fixes the absorption coefficient while letting the space (layer) thickness approach zero, one obtains the correct limit. In other words, if the layer thickness is finite while the absorption coefficient approaches zero, the approximation is invalid. If the absorption coefficient is fixed while the layer thickness approaches zero, the approximation is valid. For phonon thermal conduction, the mean free path is fixed, in other words, the absorption coefficient is fixed. The approximation method, diffusion in the layer while the jump condition is at the interface, is therefore valid for phonon thermal conduction.

IV. CONCLUSIONS

This work has presented a theoretical study on phonon heat conduction in nano- and microthin films with cylindrical

and spherical geometries. It defines heat conduction based on equilibrium temperatures at the interfaces and within the films. An approximation method, diffusion approximation or quasiequilibrium within the film, coupled with the jump boundary conditions, is applied to solve the Boltzmann transport equation for phonons. The method is validated by its approaching the limit to Fourier's law when the size of the cylinder and the sphere is in the range of that of bulk materials. It is further verified by investigating the optically thick approximation used in thermal radiation. Calculations show that a significant drop in temperature occurs at the interfaces for micro- and nanocylindrical and spherical media. For cylindrical media, the effective thermal conductivity is determined by both the film thickness and the diameter of the inner cylinder. For spherical media, the effective conductivity is mainly determined by the size of the inner sphere.

¹C. L. Tien, A. Majumdar, and F. Gerner, *Microscale Energy Transport* (Taylor and Francis, New York, 1998).

²A. Majumdar, *J. Heat Transfer* **115**, 7 (1993).

³T. Zeng and G. Chen, *J. Heat Transfer* **123**, 340 (2001).

⁴G. Chen and T. Zeng, *Microscale Thermophys. Eng.* **5**, 71 (2001).

⁵M. V. Klein, *IEEE J. Quantum Electron.* **9**, 1760 (1986).

⁶S. Tamura, Y. Tanaka, and H. J. Maris, *Phys. Rev. B* **60**, 2627 (1999).

⁷C. Weisbuch and B. Vinter, *Quantum Semiconductor Structures* (Academic, Boston, 1991).

⁸X. Duan, Y. Huang, and C. M. Lieber, *Nano Lett.* **2**, 487 (2002).

⁹Y. Wu and P. Yang, *Adv. Mater.* **13**, 520 (2001).

¹⁰R. J. Jackman, S. T. Brittain, A. Adams, M. G. Prentiss, and G. M. Whitesides, *Science* **280**, 2089 (1998).

¹¹M. Wu, Y. D. Zhang, S. Hui, T. D. Xiao, S. Ge, W. A. Hines, J. I. Budnick, and M. J. Yacaman, *J. Appl. Phys.* **92**, 6809 (2002).

¹²M. Drndic, M. V. Jarosz, N. Y. Morgan, M. A. Kastner, and M. G. Bawendi, *J. Appl. Phys.* **92**, 7498 (2002).

¹³H. B. G. Casimir, *Physica* **5**, 495 (1938).

¹⁴M. N. Ozisik, *Radiative Transfer and Interactions with Conduction and Convection* (Wiley, New York, 1973).

¹⁵M. F. Modest, *Radiative Heat Transfer* (McGraw-Hill, New York, 1993).

¹⁶G. Chen, *J. Heat Transfer* **118**, 539 (1996).

¹⁷T. Zeng and G. Chen, *J. Appl. Phys.* **92**, 3152 (2002).

¹⁸E. T. Swartz and R. O. Pohl, *Rev. Mod. Phys.* **61**, 605 (1989).